Sex-specific lipid-mediated mechanisms drive MASLD progression revealed by paired liver–blood multi-omics

Shashank Gupta[1], Oveis Jamialahmadi[2], Rosellina M. Mancina[2,3,4], Daniel Duberg[5], Umberto Vespasiani Gentilucci[4,6], Federica Tavaglione[4], Vincenzo Bruni[7], Dario Tuccinardi[7,8], Tuulia Hyötyläinen[5,*], Stefano Romeo[2,9,10,11,*], Matej Orešič[1,12,13,*]

[1]School of Medical Sciences, Faculty of Medicine and Health, Örebro University, 703 62 Örebro, Sweden.

[2]Center for Reproduction, Metabolism and Molecular Medicine (CeRM), Department of Medicine (H7), Karolinska Institute, Huddinge, 171 77 Stockholm, Sweden.

[3]Department of Life Science, Health, and Health Professions, Link Campus University, Rome, Italy.

[4]Research Unit of Clinical Medicine and Hepatology, Department of Medicine and Surgery, Università Campus Bio-Medico di Roma, Rome, Italy.

[5]School of Science and Technology, Örebro University, 70281 Örebro, Sweden.

[6]Operative Unit of Clinical Medicine and Hepatology, Fondazione Policlinico Universitario Campus Bio-Medico, Rome, Italy.

[7]Fondazione Policlinico Universitario Campus Bio-Medico, Rome, Italy.

[8]Department of Endocrinology and Diabetes, University Campus Bio-Medico of Rome, Rome, Italy.

[9]Department of Endocrinology, Karolinska University Hospital, Huddinge, Sweden.

[10]Department of Medical and Surgical Sciences, Magna Graecia University, Catanzaro, Italy.

[11]Department of Cardiology, Sahlgrenska University Hospital, 413 45 Gothenburg, Sweden.

[12]Turku Bioscience Centre, University of Turku and Åbo Akademi University, Turku 20520, Finland.

[13]Department of Life Technologies, University of Turku, Turku 20520, Finland.

*Corresponding authors and equal senior contribution

tuulia.hyotylainen@oru.se

stefano.romeo@ki.se

matej.oresic@oru.se

Abstract

Metabolic dysfunction-associated steatotic liver disease (MASLD) exhibits marked heterogeneity and sex differences, yet the molecular mechanisms underlying disease progression remain incompletely understood. Here, we present the largest integrative multi-omics study to date combining matched liver tissue and blood profiling in 211 biopsy-confirmed, morbidly obese individuals with MASLD undergoing bariatric surgery. We integrate hepatic transcriptomics, metabolomics, and lipidomics with serum metabolomics to resolve compartment-specific and sex-dependent molecular networks. Across sexes, MASLD is characterized by suppressed hepatic amino acid metabolism and extensive lipid remodeling, accompanied by inverse metabolic signatures in circulation, consistent with systemic spillover. Strikingly, disease progression in men is driven by a streamlined triacylglycerol-centric pathway that mediates transcriptional effects on steatosis and inflammation, whereas women exhibit distributed, multi-layered networks linking lipid, amino acid, and immune pathways. Mediation analyses identify hepatic lipid modules as key intermediates connecting gene expression to histopathology. These findings reveal sex-specific molecular architectures of MASLD, demonstrate that circulating biomarkers do not reflect hepatic metabolism, and provide a framework for sex-specific precision medicine.

Key words: fibrosis; inflammation; lipidomics; MASLD; metabolomics; multi-omics; sexual dimorphism; steatosis; transcriptomics.

Introduction

Metabolic dysfunction-associated steatotic liver disease (MASLD), formerly NAFLD, is the most prevalent chronic liver disease worldwide, affecting over one billion individuals and representing a leading cause of cirrhosis and hepatocellular carcinoma[1,2]. Despite this growing burden, MASLD remains biologically heterogeneous, with individuals exhibiting divergent trajectories from steatosis to inflammation and fibrosis that are incompletely understood.

A major unresolved aspect of MASLD is the pronounced sexual dimorphism in disease susceptibility and progression. Men display higher disease prevalence and increased risk of hepatocellular carcinoma, whereas women, particularly after menopause, show higher rates of advanced fibrosis and cirrhosis[3,4]. These differences are thought to arise from complex hormonal and metabolic interactions, including estrogen-mediated regulation of lipid metabolism and inflammation, and altered androgen signaling[5]. However, the molecular pathways underlying sex-specific disease trajectories remain poorly defined.

Recent advances in multi-omics technologies have enabled integrative analyses of transcriptomic, metabolomic, and lipidomic alterations in MASLD. These studies consistently implicate disrupted amino acid metabolism, bile acid signaling, and extensive lipid remodeling as central features of disease. However, most investigations rely on single tissues or circulating biomarkers, limiting insight into how hepatic molecular changes relate to systemic metabolism. Emerging evidence suggests that metabolite levels may exhibit opposing trends between liver and blood, reflecting trapping versus metabolic spillover[6,7], yet this phenomenon has not been systematically characterized in large, well-phenotyped cohorts[8,9].

Moreover, while multi-omics studies have identified associations between molecular layers and disease phenotypes, the mechanisms linking gene expression to histopathological outcomes remain largely unresolved. In particular, it is unclear which molecular processes mediate these relationships and whether such mechanisms differ between men and women[10].

Here, we address these gaps through integrative multi-omics profiling of paired liver tissue and serum from 211 biopsy-confirmed people with MASLD. By combining hepatic transcriptomics, metabolomics, and lipidomics with serum metabolomics, and applying network and mediation analyses, we define compartment-specific and sex-dependent molecular architectures of MASLD progression. We show that, while both sexes share core metabolic disruptions, disease progression in men is driven by a focused triacylglycerol-centered pathway, whereas women exhibit broader, multi-

layered networks linking lipid metabolism, amino acid catabolism, and immune regulation. Furthermore, circulating metabolites frequently display inverse patterns relative to liver tissue, underscoring the limitations of inferring hepatic biology from blood alone. Together, these findings reveal lipid-mediated, sex-specific mechanisms of MASLD progression and highlight the importance of dual-compartment multi-omics for precision medicine.

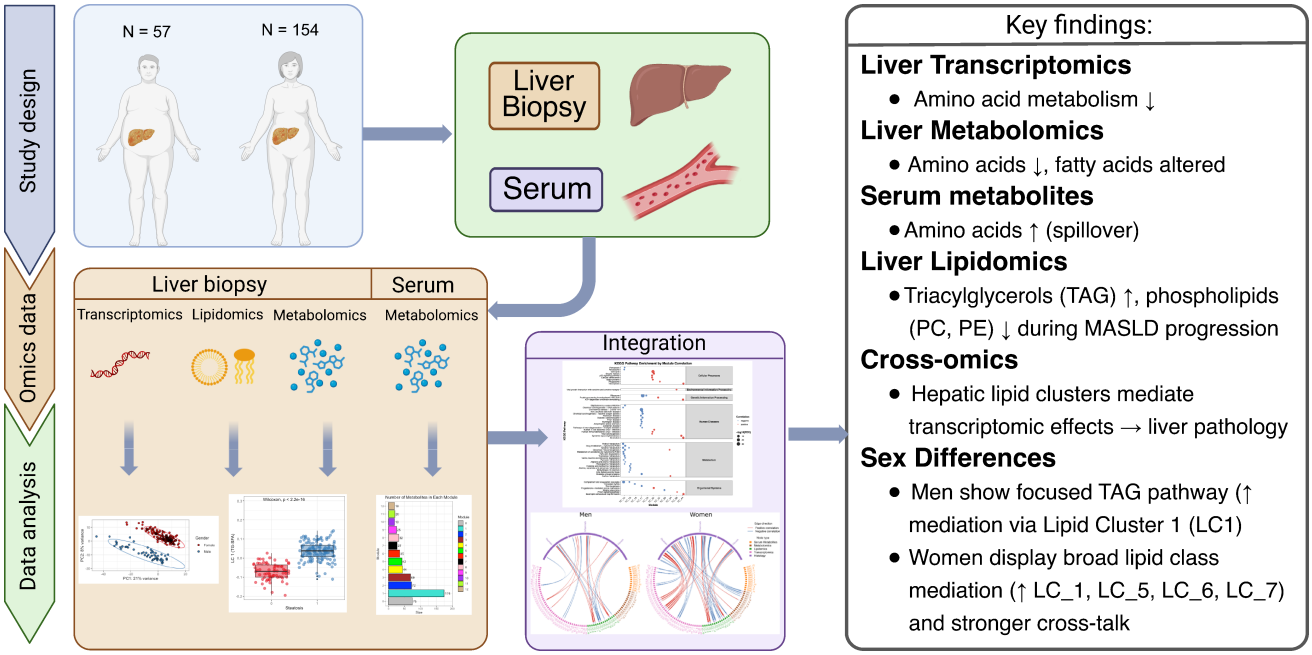

Figure. 1: Overview of the study design, omics data, and data analysis workflow in morbidly obese individuals with biopsy-confirmed MASLD undergoing bariatric surgery. The study included matched liver biopsy and serum samples collected during bariatric surgery from men (n = 57) and women (n = 154) participants. Transcriptomics, lipidomics, and metabolomics analyses were performed on liver biopsy samples, while metabolomics analysis was conducted on serum samples. The omics data were analyzed to identify differences between MASLD groups using various statistical and visualization approaches, including PCA, clustering, and pathway enrichment analysis.

Results

Cohort characteristics

Among 211 morbidly obese participants with biopsy-confirmed MASLD, men were older than women (median 48 vs. 43 years; $p = 0.009$) with similar BMI (**Table 1**). Men exhibited higher HbA1c, aminotransferases, and GGT, alongside lower HDL-cholesterol (HDL-C) and higher triglycerides (all $p < 0.05$). Steatosis and inflammation were more prevalent in men, whereas fibrosis did not differ

between sexes (**Table 1**).

Table 1. Baseline clinical and histological characteristics of the MASLD cohort stratified by sex. MASLD, metabolic dysfunction-associated steatotic liver disease; ALT, alanine aminotransferase; AST, aspartate aminotransferase; GGT, gamma-glutamyl transferase; HDL-C, high-density lipoprotein; LDL-C, low-density lipoprotein; BMI, body mass index. For continuous variables, medians and interquartile ranges (IQR) are shown; for categorical variables, frequencies are shown as n (%). Steatosis, inflammation, and fibrosis were dichotomized as "No" (grade/stage 0) and "Yes" (grade/stage ≥1). *Median (IQR); n (%). #p values were calculated using the Wilcoxon rank-sum test for continuous variables and the χ^2 test for categorical variables. Bold p values denote statistical significance at the $p < 0.05$ level.

VARIABLE	WOMEN (N=154)*	MEN (N=57)*	P VALUE#
AGE, YR	43 (35, 49)	48 (37, 54)	**0.009**
BMI, Kg/m²	41 (38, 44)	42 (39, 45)	0.300
GLUCOSE, mg/dL	98 (92, 106)	100 (95, 111)	0.079
HbA1c, %	5.50 (5.30, 5.90)	5.80 (5.40, 6.10)	**0.002**
AST, U/L	25 (20, 30)	31 (26, 37)	**<0.001**
ALT, U/L	26 (19, 39)	38 (29, 58)	**<0.001**
GGT, U/L	22 (17, 31)	31 (25, 41)	**<0.001**
TOTAL CHOLESTEROL, mg/dL	181 (164, 204)	177 (156, 191)	0.083
HDL-C, mg/dL	47 (42, 53)	39 (35, 45)	**<0.001**
LDL-C, mg/dL	122 (103, 145)	118 (104, 136)	0.300
TRIGLYCERIDES, mg/dL	122 (93, 158)	141 (97, 186)	**0.023**
STEATOSIS Yes, N (%)	89 (58%)	50 (88%)	**<0.001**
INFLAMMATION Yes, N (%)	77 (50%)	44 (77%)	**<0.001**
FIBROSIS Yes, N (%)	100 (65%)	42 (74%)	0.2

Transcriptomic shifts reflect stage-specific metabolic and inflammatory programs

Principal component analysis revealed a strong effect of sex on global transcriptomic variation (**Supplementary Fig. 1**), and all downstream analyses were adjusted accordingly. Differential expression analysis identified extensive transcriptional remodeling in steatosis and inflammation, with more limited changes in fibrosis, which should be interpreted cautiously given the smaller number of fibrosis-positive samples (**Figure 2a**, **Supplementary Table 1**). Early disease stages shared metabolic and inflammatory pathways, whereas fibrosis showed a distinct profile enriched for extracellular

matrix remodeling and immune pathways (**Figure 2b**; **Supplementary Table 2)**[11,12].

Pathway enrichment analysis demonstrated consistent downregulation of amino acid metabolism and upregulation of PI3K–Akt signaling and focal adhesion pathways (**Figure 2c**).

Fibrosis-associated genes highlighted dysregulation of mitochondrial and lipid metabolism pathways, exemplified by LIAS and LPIN1, alongside activation of immune and extracellular matrix–related genes, including FCGR1A, HPSE, IFI27, and HLA-B[13-18].

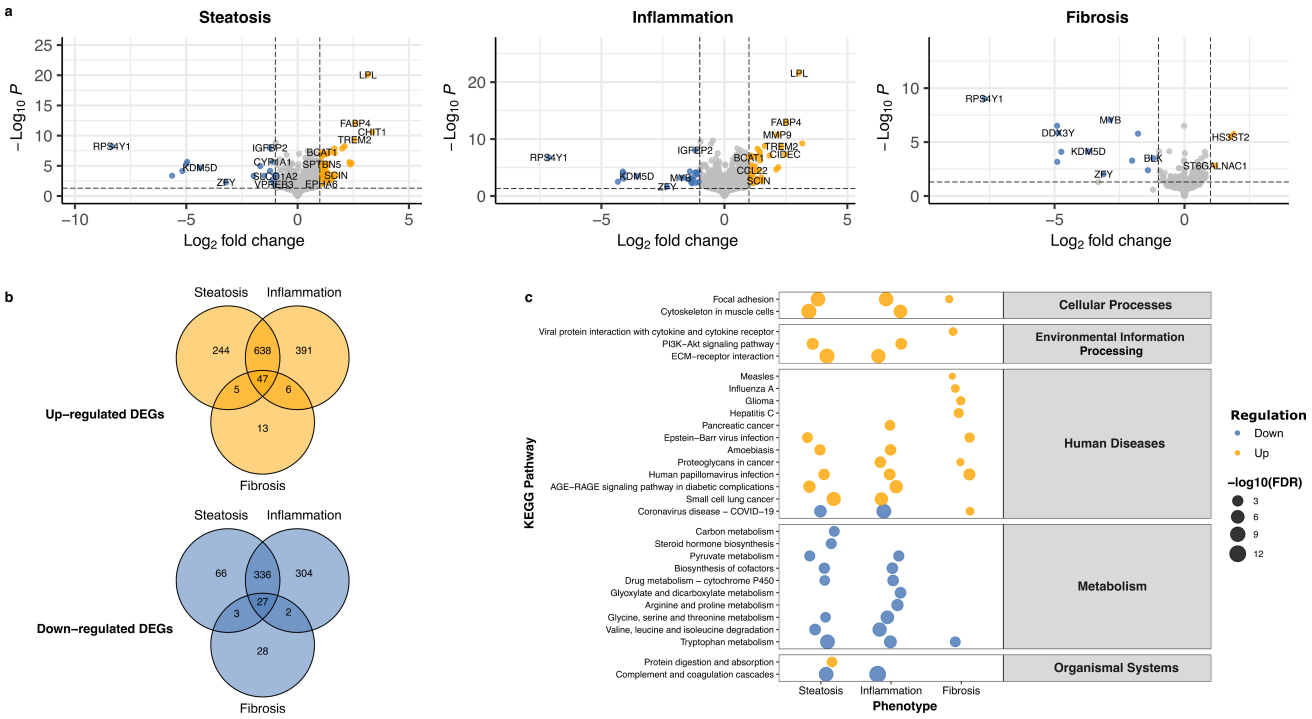

Figure 2. Differentially expressed genes (DEGs) across MASLD histological features. (**a**) Volcano plots illustrating upregulated and downregulated DEGs associated with steatosis, inflammation, and fibrosis respectively. Selected top-ranked genes are labeled. Orange and Blue color represent the significant up and down regulated genes respectively. (**b**) Venn diagram showing the overlap of DEGs across the three histological features. Inflammation displayed the largest number of unique and shared DEGs, while fibrosis contributed comparatively fewer, consistent with a more specialized transcriptional program. (**c**) KEGG pathway enrichment of up- and downregulated DEGs across features. Upregulated pathways were predominantly immune- and inflammation-related, including PI3K–Akt signaling, focal adhesion, and complement and coagulation cascades, whereas downregulated DEGs were enriched in amino acid and lipid metabolism pathways.

Integrated metabolomic and lipidomic remodeling mirrors transcriptional changes

Liver metabolomics and lipidomics revealed extensive metabolic remodeling across MASLD stages

(Figure 3, **Supplementary Tables 3–4**). Steatosis and inflammation were characterized by depletion of amino acids and polyunsaturated fatty acids, alongside increased bile acids, indicating impaired nitrogen metabolism and altered lipid signaling. Lipidomic changes were dominated by accumulation of triacylglycerols and depletion of membrane lipids, including phosphatidylcholines, sphingomyelins, and ceramides. These alterations closely paralleled transcriptomic patterns. Joint pathway analysis confirmed coordinated disruption of glycolysis, linoleic acid metabolism, and tryptophan metabolism (**Supplementary Fig. 2**).

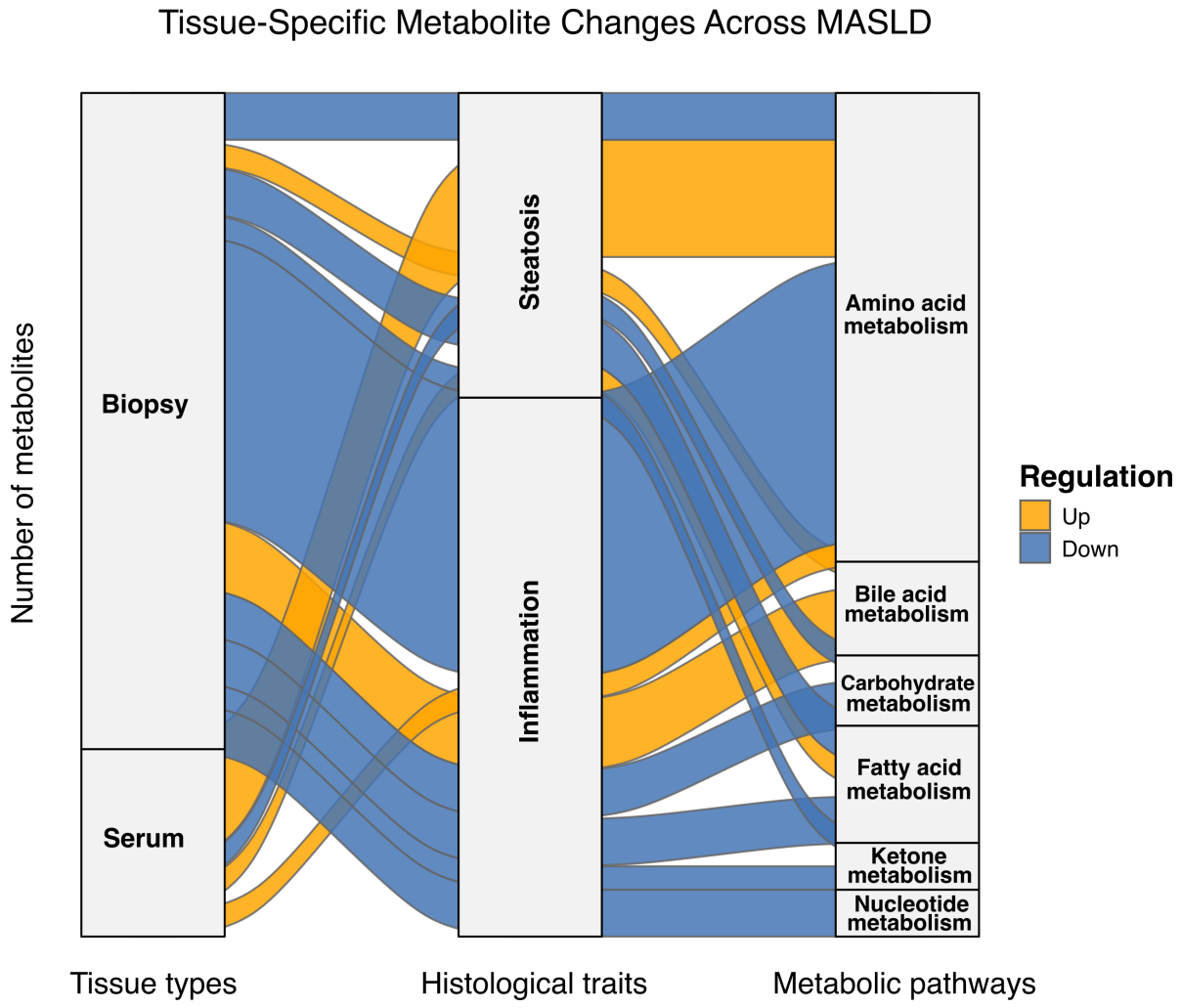

Figure 3. Sankey plot of differential metabolite regulation across MASLD histological features. The Sankey diagram illustrates the flow of significantly altered metabolites (FDR ≤ 0.1) across tissue type (Serum, Biopsy), histological phenotype (Inflammation, Steatosis), and metabolic pathway annotation. Each stream represents the number of unique metabolites linking these categories. Upregulated metabolites are shown in orange, while downregulated metabolites are shown in blue. Metabolic pathways were annotated into major classes, including amino acid metabolism, fatty acid metabolism, bile acid metabolism, nucleotide metabolism,

carbohydrate metabolism, and ketone metabolism; unclassified or putative metabolites were removed from the plot. Biopsy-derived profiles displayed broader metabolic alterations than serum, with dominant changes in amino acid and bile acid metabolism in inflammation, and in amino acid and fatty acid metabolism in steatosis. Notably, amino acid metabolism showed divergent trends across tissues: while hepatic (biopsy) metabolites were largely downregulated, serum metabolites exhibited consistent upregulation, highlighting tissue-specific and inverse regulation of amino acid metabolism in MASLD.

Liver and blood metabolomes are inversely regulated

Serum metabolomics showed an inverse pattern to liver tissue (**Figure 3**, **Supplementary Table 5**), with amino acids and related metabolites decreased in the liver but increased in circulation, consistent with impaired hepatic metabolism and escape of metabolites into the bloodstream; a similar pattern was observed for bile acid–related pathways. This liver–blood discordance was consistent across sexes but more pronounced in women, in line with broader systemic metabolic remodeling. These findings support compartment-specific metabolic regulation[6,7] and highlight limitations of inferring hepatic metabolism from circulating biomarkers[8,9].

Sex-specific molecular architectures define MASLD progression

Integrative network analysis revealed marked sexual dimorphism in MASLD molecular organization (**Figure 4**, **Supplementary Table 6**). Consistent with this, sex-stratified analyses showed that lipid accumulation was more tightly associated with disease severity in men, whereas women exhibited broader perturbations across metabolic pathways. In men, disease progression was characterized by a focused lipid-centric architecture, with triacylglycerol-rich modules strongly associated with steatosis and inflammation and limited cross-omic connectivity (**Figure 4a**). This is consistent with human genetics showing a causal role of triglycerides accumulation on MASLD progression[19].

In contrast, women exhibited highly interconnected multi-omic networks linking lipid metabolism, amino acid catabolism, and immune signaling (**Figure 4b**). Lipid modules enriched in phosphatidylcholine and phosphatidylethanolamine (e.g., LC_7 and LC_10) were strongly associated with amino acid–related metabolite modules (e.g., MC_3) (**Figure 4d, Supplementary Fig. 3, Supplementary Table 7**). In parallel, transcriptomic programs, including PPAR signaling, were associated with disease traits and pathway enrichment patterns (**Figure 4c**). Cross-omic correlations were more numerous and stronger in women (**Supplementary Fig. 3**), indicating coordinated multi-layer remodeling.

These findings indicate that MASLD progression in men follows a streamlined lipid-driven trajectory, whereas in women MASLD progression is the result of a more complex metabolic and immune perturbation.

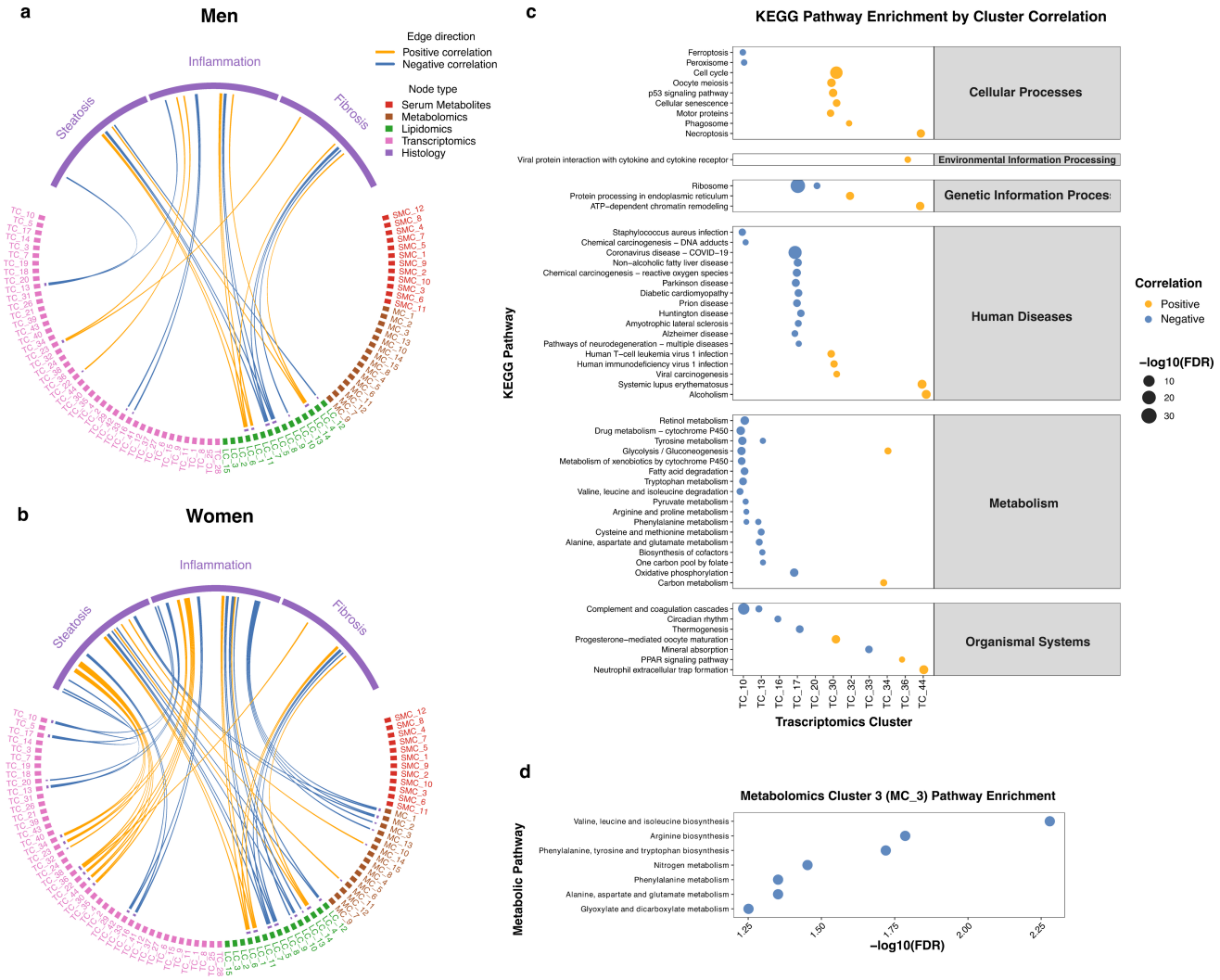

Figure 4. Histology–omics associations and transcriptomic pathway enrichment in men and women. (a–b) Chord diagrams of significant Spearman correlations (FDR ≤ 0.1) between histological features (steatosis, inflammation, fibrosis) and module eigengenes from liver metabolomics (MC), lipidomics (LC), transcriptomics (TC), and serum metabolomics (SMC). Node colors indicate data source (red = SMC, brown = MC, green = LC, pink = TC, purple = histology), and edge colors indicate correlation direction (orange = positive, blue = negative). Correlations among omics layers (MC, LC, and TC) are presented separately in **Supplementary Fig. 3**. Women (b) exhibited more associations than men (a), suggesting stronger multi-omic links to histology. (c) KEGG pathway enrichment of transcriptomic modules associated with histological traits. Modules (x-axis, "TC_#") are shown with enriched KEGG pathways (y-axis), grouped by functional category. Point size reflects

the number of genes, and color indicates correlation direction (orange = positive, blue = negative). Only pathways with FDR ≤ 0.1 are displayed. (d) Bubble plot showing significantly enriched metabolic pathways (FDR ≤ 0.1) for metabolites in MC_3. Each dot represents a pathway, with its position along the x-axis corresponding to the significance level (-log10 FDR). Larger values along the x-axis indicate higher significance. Only pathways passing the FDR ≤ 0.1 are displayed.

Lipid mediation defines sex-specific mechanisms linking transcription to disease

Mediation analysis identified lipid modules as the primary intermediaries linking transcriptional programs to histological outcomes (**Figure 5**; **Supplementary Tables 8–9**). In men, a single triacylglycerol/diacylglycerol module (LC1) mediated nearly the entire effect of multiple transcriptomic programs on steatosis and inflammation (**Figure 5a)**, indicating a dominant neutral-lipid pathway.

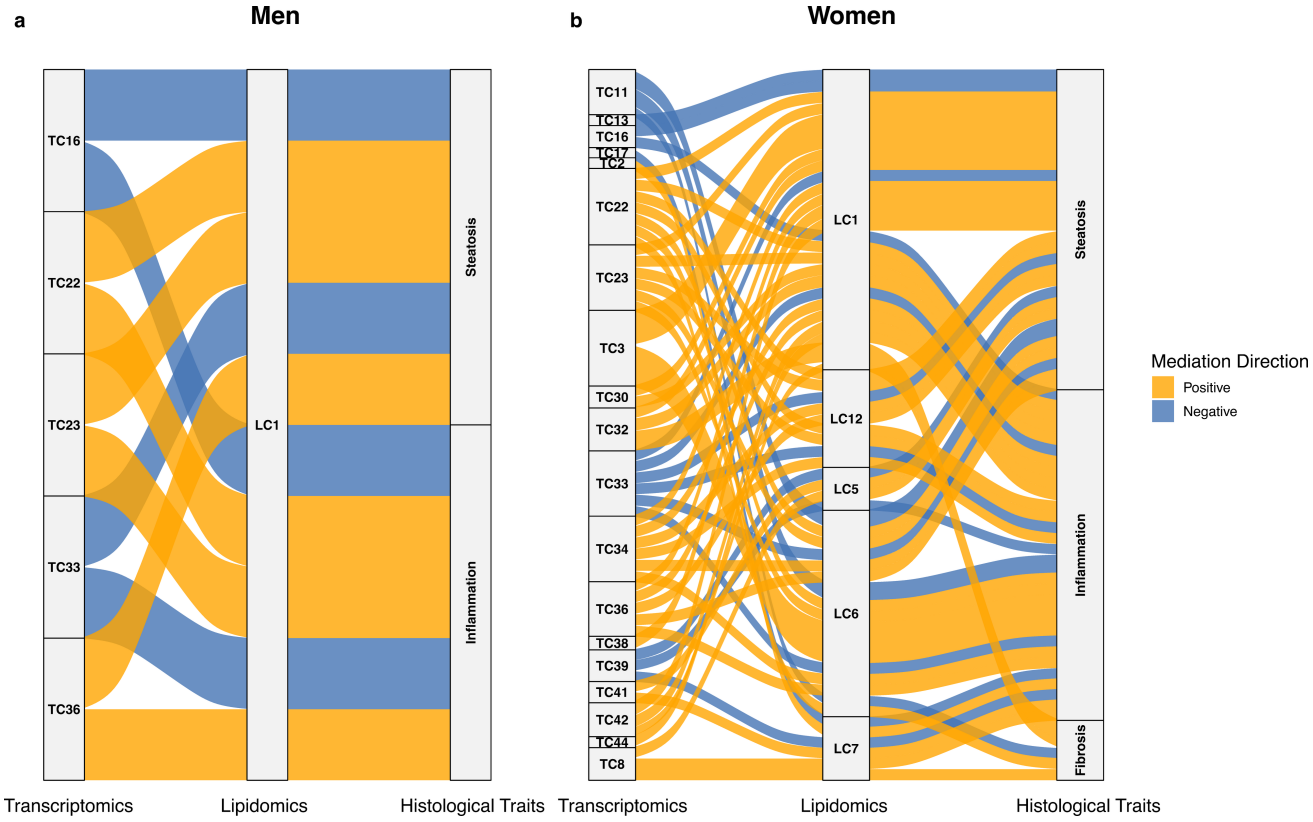

Figure 5. Sex-stratified mediation analysis of transcriptomic and lipid modules on MASLD outcomes. The alluvial plots display significant mediation effects (ACME FDR ≤ 0.1 and proportion mediated > 0) in men (panel a) and women (panel b). Transcriptomic modules (left axis) are connected to lipid (LC) mediator modules (middle axis), which in turn connect to MASLD outcomes (Steatosis, Inflammation, Fibrosis; right axis). The width of each flow represents the proportion of the total effect mediated, with red indicating positive mediation

and blue indicating negative mediation. Stratum labels highlight the module and outcomes involved. These plots illustrate sex-specific pathways in which transcriptomic alterations influence MASLD outcomes through lipid mediators, revealing mechanistic differences between males and females in disease progression.

In women, mediation was distributed across multiple lipid modules, including both neutral and membrane lipids, linking transcriptional programs to disease phenotypes through broader metabolic pathways (**Figure 5b**).

These results establish lipid remodeling as a central mechanistic driver of MASLD and reveal distinct sex-specific mediation architectures.

Discussion

The main findings of this work are that MASLD is characterized by coordinated suppression of amino acid metabolism and lipid remodeling; circulating metabolites exhibit inverse relationships with hepatic metabolism; and disease progression follows sex-specific perturbation of the liver homeostasis.

A central finding is the divergence in disease mechanisms between sexes. In men, MASLD progression is driven by a focused triacylglycerol-centered pathway that mediates transcriptional effects on steatosis and inflammation. In contrast, women exhibit a broader perturbation adding to lipid metabolism also amino acid metabolism and immune signaling perturbation. Mediation analysis further identifies lipid remodeling as a central mechanism linking gene expression to disease phenotypes. The near-complete mediation by a single triacylglycerol module in men contrasts with a distributed mediation architecture in women involving multiple lipid classes. Taken all this together, results indicate that MASLD heterogeneity is, at least in part, explained by the disease being a sex-specific liver perturbation contributing to clinical difference in the course of the diseases between men and women[20,21]. These differences suggest distinct therapeutic needs with a focused lipid targeting in men and a broader pathway modulation in women. Hormonal regulation likely contributes to these patterns. Estrogen modulates lipid metabolism and inflammation[22,23], whereas androgen imbalance is associated with MASLD risk[24,25], potentially contributing to shape the observed sex-specific molecular networks.

A second key observation is the discordance between liver and blood metabolomes. Amino acids and bile acids–related metabolites were depleted in liver but elevated in circulation, indicating leaking or active secretion of metabolites rather than a direct reflection of their retention. This finding supports compartment-specific metabolic regulation[6,7] and highlights a limitation of circulating biomarkers as proxies for liver metabolism[8,9].

Strengths of this study include biopsy-confirmed disease, the large number of women in the study, paired tissue–blood multi-omics, and integrative analyses enabling mechanistic inference. Limitations include the cross-sectional design, restriction to people with obesity although this could also be seen as an advantage because it allows us to investigate a system under metabolic stress. In addition, fibrosis-related analyses should be interpreted with caution, as the study may have been underpowered to detect more subtle fibrosis-associated transcriptomic changes. Moreover, residual confounding from unmeasured exposures cannot be excluded[26,27].

In conclusion, MASLD progression is driven by lipid-mediated perturbation that differs between sexes and cannot be inferred from circulating biomarkers alone. These findings support a shift toward tissue-informed and sex-specific approaches to MASLD biology and investigation of therapeutics in studies stratified by sex.

Methods

Study design and participants

This study included 211 persons, consisting of 154 women and 57 men, with biopsy-confirmed MASLD from the MAFALDA study[28,29]. Briefly, consecutive individuals with morbid obesity eligible for bariatric surgery were recruited from May 2020 to June 2021 at Fondazione Policlinico Universitario Campus Bio-Medico, Rome, Italy. At the time of bariatric surgery, matched liver tissue and serum samples were collected from each individual for multi-omics profiling. Transcriptomics, lipidomics, and metabolomics datasets were generated from liver biopsies, while serum metabolomics provided the systemic perspective. Participants were stratified by histological features, namely steatosis, inflammation, and fibrosis, according to liver pathology.

The study has been approved by the Local Research Ethics Committee at Campus Bio-Medico University Hospital (approval no. 16/20), and by the Swedish Ethics Review Authority (Dnr 2025-08073-01), and it was conducted in accordance with the principles of the Declaration of Helsinki. All participants gave written informed consent to the study.

Lipidomics and analysis of polar and semipolar metabolites

The samples were randomized and two methods were applied for separate extraction of lipids and polar/semipolar metabolites, and the extracts were then analyzed using an ultra-high-performance liquid chromatography quadrupole time-of-flight mass spectrometry (UHPLC-QTOFMS) as described

in **Supplementary Table 10**.

The lipidomic analyses were done using method described earlier (Agilent Technologies, Santa Clara, CA, USA) as described previously[30]. Internal standard mixture was used for normalization and lipid-class specific calibration was used for quantitation. MS data processing was performed using open-source software MZmine v. 4.3[31] as described below. The identification was done with a custom database, with identification levels 1 and 2 based on the Metabolomics Standards Initiative[32]. However, it should be noted that the method cannot distinguish isomers differing only by their double bond position. Quantification of lipids was performed using a 7-point internal calibration curve (0.1–5 µg/mL). Quality control was performed throughout the dataset by including blanks, pure standard samples, extracted standard samples, and control plasma samples. The RSD of lipids in the pooled plasma samples (n = 9) was on average 16.8%.

The analysis of polar and semipolar metabolites was performed with a method described in[33]with an internal standard mixture used for normalization and calibration curves established for bile acids and amino acids as previously described. Identification was based on an in-house spectral library combined with external databases, with identification levels 1 and 2 based on the Metabolomics Standards Initiative[32]. Quality control was performed throughout the dataset by including blanks, pure standard samples, extracted standard samples, and control plasma samples. The RSD of metabolites in the pooled plasma samples (n = 9) was on average 20.5%.

Data preprocessing for metabolomics

The raw data was first converted to mzML format using MS convert in ProteoWizard 3.0[34]. Mass spectrometry data processing was performed using the open-source software package MZmine 4.3[31]. The following steps were applied in this processing: (i) crop filtering with a m/z range of 350–1200 m/z and an RT range of 2.0 to 12 min; (ii) mass detection with a noise level of 750; (iii) chromatogram builder with a minimum time span of 0.08 min, minimum height of 1000 and a m/z tolerance of 0.006 m/z or 10.0 ppm; (iv) chromatogram deconvolution using the local minimum search algorithm with a 70 % chromatographic threshold, 0.05 min minimum RT range, 1000 minimum absolute height, a minimum ratio of peak top/edge of 1.7 and a peak duration range of 0.08–1.0; (v) isotopic peak grouper with a m/z tolerance of 5.0 ppm, RT tolerance of 0.05 min, maximum charge of 2 and with the most intense isotope set as the representative isotope; (vi) join aligner with a m/z tolerance of 0.007 or 7.0 ppm and a weight for of 3, a RT tolerance of 0.15 min and a weight of 1 and with no requirement of

charge state or ID and no comparison of isotope pattern; (vii) peak list row filter with a minimum of 10 % of the samples; (vii) gap filling using the same RT and m/z range gap filler algorithm with an m/z tolerance of 0.009 m/z or 11.0 ppm; (ix) identification of metabolites was done using a custom database, constructed by analyzing authentic standards with m/z information and retention time information adjusted with internal standards, with an m/z tolerance of 0.009 m/z or 10.0 ppm and a RT tolerance of 0.25 min; and, (xi) normalization using the internal standard with closest retention time.

Transcriptomics analyses

Raw RNA-seq reads were aligned to the reference genome using STAR[35], followed by transcript quantification with RSEM[36]. The resulting gene-level count matrix was normalized to account for sequencing depth and transcript length. Genes with low expression (fewer than ten counts per million per sample on average) were filtered out, and the count per million table was VST normalized using DeSeq2[37]. After final filtering and normalization, the dataset comprised 29,323 genes for men and 33,601 genes for women. Differential expression analysis was done using DeSeq2.

Covariates

Relevant clinical covariates including age, sex, and body mass index (BMI) were incorporated in all downstream analyses to account for potential confounders. For linear and logistic regression analyses, age and BMI were entered as continuous covariates, and biological sex was included as a categorical variable. In network, correlation, and mediation analyses, these variables were consistently adjusted to ensure observed molecular associations reflected true biological differences rather than confounding demographic or metabolic factors.

Statistical analysis

All statistical analyses were conducted in the R statistical programming environment (version 4.4.1). Preprocessing of metabolomics, and lipidomics data involved replacing zero values with imputed half-minimums for each respective feature, followed by log2 transformation and autoscaling. Clustering of the metabolite, lipid, and transcriptomic data was performed using weighted gene co-expression network analysis (WGCNA) with biweight midcorrelation. Module eigengenes were computed and correlated with clinical and molecular variables using pairwise Spearman correlation, with p-values adjusted by the FDR method. Metabolic pathway enrichment analyses were done in MetaboAnalyst 5.0[38], while transcriptomic module enrichment was determined using KEGG pathway analysis via the

clusterProfiler R package[39].

Mediation analysis was performed with the mediation R package in a two-step procedure. First, a linear model regressed each mediator (lipid or metabolite module) on each transcriptomic module, while adjusting for age and BMI. Second, a logistic regression model regressed the binary clinical outcome (steatosis, inflammation, or fibrosis) on both the transcriptomic module and the mediator, also adjusting for age and BMI. The mediate function estimated the average causal mediation effect (ACME), the average direct effect (ADE), and the proportion of the total effect that was mediated, using 1,000 bootstrap simulations to obtain confidence intervals and p-values. All p-values were FDR adjusted, and only pathways or mediation effects with ACME FDR < 0.05 and proportion mediated > 0 were considered statistically significant.

Network analysis

Weighted Gene Co-expression Network Analysis (WGCNA) was performed using the blockwiseModules function in the WGCNA R package[40]. Analysis parameters included biweight midcorrelation (corType = 'bicor') to account for outliers, signed correlation networks (TOMtype and networkType = 'signed'), and a sensitive module detection parameter (deepSplit = 2). Module sizes were set to a minimum of 20 genes (minModuleSize = 20), and the merging threshold for similar modules was adjusted to mergeCutHeight = 0.2. Default settings were used for other parameters.

Module eigengenes (MEs) were computed as the first principal component of the expression profiles for each module. The relatedness between modules was examined through eigengene network clustering. MEs were correlated with clinical and molecular variables using Spearman's correlation, and p-values were adjusted for multiple comparisons using the false discovery rate (FDR).

Author contributions

Conceptualization and design of study (TH, SR, MO), clinical study (OJ, RMM, UMG, FT, VB, DT, SR), metabolomics analysis (DD, TH, MO), data analysis and interpretation (SG, with critical input from RMM, TH, SR, MO), manuscript preparation (SG, TH, MO), critical review and editing (all authors).

Funding

M.O. and T.H. were supported by the "Investigation of endocrine-disrupting chemicals as contributors

to progression of metabolic dysfunction-associated steatotic liver disease" (EDC-MASLD) consortium funded by the Horizon Europe Program of the European Union under Grant Agreement 101136259. Views and opinions expressed are those of the authors only and do not necessarily reflect those of the European Union. Neither the European Union nor the granting authority can be held responsible for them. S.R. was supported by the Region Stockholm (ALF project grant, FoUI-1021801), the Swedish Cancerfonden (22 2270 Pj), the Swedish Research Council (Vetenskapsradet (VR), 2023-02079), the Swedish state under the Agreement between the Swedish government and the county councils (the ALF agreement, ALFGBG-965360), the Swedish Heart Lung Foundation (20220334), the Novonordisk Distinguished Investigator Grant - Endocrinology and Metabolism (NNF23OC0082114), the Novonordisk Project grants in Endocrinology and Metabolism (NNF24OC0091535, and a Novo Nordisk donation to the Karolinska Institutet in connection with the professor appointment.

Acknowledgments

The authors thank Lucas Landmann, Maelle Uler, and Kattis Kristofferson for assistance in metabolomics analysis.

Data availability statement

Data from the clinical study are available upon request and an appropriate institutional collaboration agreement.

Conflicts of interest

In the last 5 years S.R. received research grants from Novonordisk and AstraZeneca for basic science research on steatotic liver disease, and has been consulting for AstraZeneca, GSK, Celgene Corporation, Ribocure AB¸ Madrigal, Ultragenyx, Amgen, Sanofi, Wave Life Sciences, Lipigon, Novartis, Profluent, Aina, Echosense and Chiesi; declares equity from Heptabio; and is inventor on a Patent with title "Method for treating fatty liver disease", on PSD3, US application number 17,480266 filed on 21st September 2021. Other authors have no conflict of interest to declare.

References

1. Kan, C., *et al.* Global burden and future trends of metabolic dysfunction-associated Steatotic liver disease: 1990-2021 to 2045. *Ann Hepatol* **30**, 101898 (2025).

2. Miller, D.M., McCauley, K.F. & Dunham-Snary, K.J. Metabolic Dysfunction-Associated Steatotic Liver Disease (MASLD): Mechanisms, Clinical Implications and Therapeutic Advances. *Endocrinol Diabetes Metab* **8**, e70132 (2025).
3. Feng, G.*, et al.* Global burden of metabolic dysfunction-associated steatotic liver disease, 2010 to 2021. *JHEP Rep* **7**, 101271 (2025).
4. Hutchison, A.L., Tavaglione, F., Romeo, S. & Charlton, M. Endocrine aspects of metabolic dysfunction-associated steatotic liver disease (MASLD): Beyond insulin resistance. *J Hepatol* **79**, 1524-1541 (2023).
5. Weiskirchen, R. & Lonardo, A. Sex Hormones and Metabolic Dysfunction-Associated Steatotic Liver Disease. *Int J Mol Sci* **26**(2025).
6. Castane, H.*, et al.* Multi-omics profiling reveals altered mitochondrial metabolism in adipose tissue from patients with metabolic dysfunction-associated steatohepatitis. *EBioMedicine* **111**, 105532 (2025).
7. Masoodi, M.*, et al.* Metabolomics and lipidomics in NAFLD: biomarkers and non-invasive diagnostic tests. *Nat Rev Gastroenterol Hepatol* **18**, 835-856 (2021).
8. Meijnikman, A.S.*, et al.* A systems biology approach to study non-alcoholic fatty liver (NAFL) in women with obesity. *iScience* **25**, 104828 (2022).
9. Bourganou, M.V.*, et al.* Unraveling Metabolic Dysfunction-Associated Steatotic Liver Disease Through the Use of Omics Technologies. *Int J Mol Sci* **26**(2025).
10. Goodrich, J.A.*, et al.* Integrating Multi-Omics with environmental data for precision health: A novel analytic framework and case study on prenatal mercury induced childhood fatty liver disease. *Environ Int* **190**, 108930 (2024).
11. Cazanave, S.*, et al.* The Transcriptomic Signature Of Disease Development And Progression Of Nonalcoholic Fatty Liver Disease. *Sci Rep* **7**, 17193 (2017).
12. Govaere, O.*, et al.* Transcriptomic profiling across the nonalcoholic fatty liver disease spectrum reveals gene signatures for steatohepatitis and fibrosis. *Sci Transl Med* **12**(2020).
13. Liu, F.*, et al.* Lipoic acid in metabolic dysfunction-associated steatotic liver disease: a review. *Nutr Metab (Lond)* **22**, 56 (2025).
14. Jang, C.H.*, et al.* The Role of Lipin-1 in the Regulation of Fibrogenesis and TGF-beta Signaling in Hepatic Stellate Cells. *Toxicol Sci* **153**, 28-38 (2016).
15. Schwinghammer, U.A.*, et al.* alpha2-Adrenergic Receptor in Liver Fibrosis: Implications for the Adrenoblocker Mesedin. *Cells* **9**(2020).
16. Bao, H.*, et al.* Integrated bioinformatics and machine-learning screening for immune-related genes in diagnosing non-alcoholic fatty liver disease with ischemic stroke and RRS1 pan-cancer analysis. *Front Immunol* **14**, 1113634 (2023).
17. Hu, Q., Luo, Y., He, H., Chen, H. & Liao, D. Comprehensive analysis of shared risk genes and immunity-metabolisms between non-alcoholic fatty liver disease and atherosclerosis via bulk and single-cell transcriptome analyses. *Heliyon* **10**, e35453 (2024).
18. Karrar, A.*, et al.* Analysis of human leukocyte antigen allele polymorphism in patients with non alcoholic fatty liver disease. *Medicine (Baltimore)* **98**, e16704 (2019).
19. Mancina, R.M., Valenti, L. & Romeo, S. Human genetics of steatotic liver disease: insights into insulin resistance and lipid metabolism. *Nat Metab* **7**, 2199-2211 (2025).
20. Loomba, R., Friedman, S.L. & Shulman, G.I. Mechanisms and disease consequences of nonalcoholic fatty liver disease. *Cell* **184**, 2537-2564 (2021).
21. Cherubini, A., Della Torre, S., Pelusi, S. & Valenti, L. Sexual dimorphism of metabolic dysfunction-associated steatotic liver disease. *Trends Mol Med* **30**, 1126-1136 (2024).
22. Alves, E.S.*, et al.* Hepatic Estrogen Receptor Alpha Overexpression Protects Against Hepatic Insulin Resistance and MASLD. *Pathophysiology* **32**(2025).
23. Kim, S.E., Min, J.S., Lee, S., Lee, D.Y. & Choi, D. Different effects of menopausal hormone therapy on non-alcoholic fatty liver disease based on the route of estrogen administration. *Sci Rep* **13**, 15461 (2023).
24. Song, M.J. & Choi, J.Y. Androgen dysfunction in non-alcoholic fatty liver disease: Role of sex hormone binding globulin. *Front Endocrinol (Lausanne)* **13**, 1053709 (2022).

25. Sarkar, M. Testosterone Levels in Women: Implications for Fatty Liver and Beyond. *J Womens Health (Larchmt)* **28**, 1015-1016 (2019).
26. Santos, A.A.*, et al.* Spatial metabolomics and its application in the liver. *Hepatology* **79**, 1158-1179 (2024).
27. Deslande, M.*, et al.* Intrahepatic levels of microbiome-derived hippurate associates with improved metabolic dysfunction-associated steatotic liver disease. *Mol Metab* **92**, 102090 (2025).
28. Tavaglione, F.*, et al.* Accuracy of controlled attenuation parameter for assessing liver steatosis in individuals with morbid obesity before bariatric surgery. *Liver Int* **42**, 374-383 (2022).
29. Raverdy, V.*, et al.* Data-driven cluster analysis identifies distinct types of metabolic dysfunction-associated steatotic liver disease. *Nat Med* **30**, 3624-3633 (2024).
30. McGlinchey, A.J.*, et al.* Metabolic signatures across the full spectrum of non-alcoholic fatty liver disease. *JHEP Rep* **4**, 100477 (2022).
31. Schmid, R.*, et al.* Integrative analysis of multimodal mass spectrometry data in MZmine 3. *Nat Biotechnol* **41**, 447-449 (2023).
32. Members, M.S.I.B.*, et al.* The metabolomics standards initiative. *Nat Biotechnol* **25**, 846-848 (2007).
33. Hyotylainen, T.*, et al.* Cord serum metabolic signatures of future progression to immune-mediated diseases. *iScience* **26**, 106268 (2023).
34. Chambers, M.C.*, et al.* A cross-platform toolkit for mass spectrometry and proteomics. *Nat Biotechnol* **30**, 918-920 (2012).
35. Dobin, A.*, et al.* STAR: ultrafast universal RNA-seq aligner. *Bioinformatics* **29**, 15-21 (2013).
36. Li, B. & Dewey, C.N. RSEM: accurate transcript quantification from RNA-Seq data with or without a reference genome. *BMC Bioinformatics* **12**, 323 (2011).
37. Love, M.I., Huber, W. & Anders, S. Moderated estimation of fold change and dispersion for RNA-seq data with DESeq2. *Genome Biol* **15**, 550 (2014).
38. Pang, Z.*, et al.* MetaboAnalyst 5.0: narrowing the gap between raw spectra and functional insights. *Nucleic Acids Res* **49**, W388-W396 (2021).
39. Yu, G., Wang, L.G., Han, Y. & He, Q.Y. clusterProfiler: an R package for comparing biological themes among gene clusters. *OMICS* **16**, 284-287 (2012).
40. Langfelder, P. & Horvath, S. WGCNA: an R package for weighted correlation network analysis. *BMC Bioinformatics* **9**, 559 (2008).